Giant resonances in exotic spherical nuclei within the RPA approach with the Gogny force

S. Péru[1,a], J.F. Berger[1], and P.F. Bortignon[2]

[1] DPTA/Service de Physique Nucléaire, BP 12, F-91680 Bruyères-le-Châtel, France
[2] Dipartimento di Fisica, Università di Milano and INFN, Via Celoria 16, I-20133 Milano, Italy

Abstract. Theoretical results for giant resonances in the three doubly magic exotic nuclei ^{78}Ni, ^{100}Sn and ^{132}Sn are obtained from Hartree-Fock (HF) plus Random Phase Approximation (RPA) calculations using the D1S parameterization of the Gogny two-body effective interaction. Special attention is paid to full consistency between the HF field and the RPA particle-hole residual interaction. The results for the exotic nuclei, on average, appear similar to those of stable ones, especially for quadrupole and octupole states. More exotic systems have to be studied in order to confirm such a trend. The low energy of the monopole resonance in ^{78}Ni suggests that the compression modulus in this neutron-rich nucleus is lower than the one of stable ones.

PACS. 21.10.Re Collective levels – 24.30.Cz Giant resonances – 21.60.Jz Hartree-Fock and random-phase approximations – 23.20.Lv γ transitions and level energies

1 Introduction

Giant multipole resonances (GR) are collective excitations of nuclei that lie at excitation energies above the nucleon separation energy (8–10 MeV), have different multipolarities and carry different spin-isospin quantum numbers. They have been observed for stable nuclei throughout the mass table with large cross-sections, close to the maximum allowed by sum rule arguments, implying that a large number of nucleons participate in a very collective nuclear motion [1,2]. It is a challenge both to experimentalists and theorists to study the properties of these states for nuclei far from the valley of stability. Not too much has been done from the experimental side yet: let us just mention the two measurements of the electric dipole GR (GDR) made in neutron-rich oxygen isotopes [3,4]. Beside GR, there are also low-lying collective excitations, in particular quadrupole and octupole states, which reflect much more than the GR the detail of shell structure. More experimental data are available for such states [5] in the case of unstable nuclei, giving us information on the modifications of the shell structure far from stability.

From the theoretical side, more and more calculations of GR and low-lying states are performed nowadays in the framework of microscopic HF + RPA or HFB + QRPA approaches. The effective nucleon-nucleon interactions used

are taken as non-relativistic effective two-body potentials [6] or relativistic Lagrangians for meson exchange [7]. Such microscopic approaches, although less accurate than more phenomenological ones, usually describe reasonably well the properties of these states in stable nuclei.

Among the effective forces used in the non-relativistic approaches, the Gogny force [8,9] is one of those which has been extensively employed for the description of GR and low-lying states in doubly closed shell nuclei with the RPA method [10–12]. Recently, this force has been used for the first time in full Quasi-Particle RPA (QRPA) calculations. Chains of isotopes in the oxygen, nickel and tin regions have been studied in order to derive the properties of low-lying states [13].

The purpose of this paper is to present the results of calculations performed in three spherical exotic nuclei: ^{78}Ni, ^{100}Sn and ^{132}Sn, and to compare them with those obtained in stable nuclei. More precisely, GR and low-lying states in these nuclei will be analyzed and comparisons will be made with systematics and with analogous quantities in the well-known ^{208}Pb. The latter nucleus will serve as a reference and, for this reason, results for ^{208}Pb will be displayed along with those of the three exotic nuclei in most tables and figures. Let us point out that the results presented here for ^{208}Pb are new. They have been derived with the D1S parameterization of the Gogny force which is the one currently used now. They slightly differ from

a e-mail: sophie.peru-desenfants@cea.fr

those of ref. [10], where the older parameterization D1 was employed.

A point we pay special attention to in the present work is the effect of the full consistency of the residual particle-hole (p-h) interaction with the mean field produced by the same force, as allowed by the use of consistently combined HF and RPA approaches. In order to analyze this effect, we present results where different components of the residual p-h interaction such as those generated by the spin-orbit or the Coulomb force are switched off. As will be seen, the influence of these often omitted components is far from being negligible.

In the following section details concerning the parameters of the two-body force, the numerical methods used for solving the RPA equations are briefly recalled along with a few useful formulas. Results are presented and discussed in sect. 3. The main conclusions of this work are summarized in sect. 4. Let us mention that a preliminary account of the present results has appeared in the workshop proceedings of ref. [14].

2 The HF + RPA approach with the Gogny force

The RPA approach employed here is described in refs. [11, 10,12]. The effective force D1S proposed by Gogny [8,9] is used. This finite-range density-dependent interaction describes the mean field of the nucleus, and the residual interaction in the RPA calculations is obtained via the functional second derivative of the mean field with respect to the one-body density matrix. We want to stress that all the terms of the effective force are considered in the HF mean-field and in the residual p-h interaction, including the spin-spin component, the Coulomb force and the terms produced by the two-body spin-orbit interaction. Only the two-body terms coming from the two-body center-of-mass correction are not included in the RPA matrix elements. Therefore, they have been also left out from the mean-field calculations. In order to get the same binding energies and radii as with the two-body center-of-mass correction, the coefficient of the spin-orbit component of D1S has been reduced from 130 MeV to 115 MeV. Such a procedure was previously employed in calculations with the D1 force, as explained in ref. [8]. The Gogny force D1S including this change of the spin-orbit strength will be called D1S′.

In the results presented here, spherical symmetry is imposed. Consequently, nuclear states can be characterized by their angular momentum J and their parity π. The individual Hartree-Fock wave functions are expanded on finite sets of spherical harmonic oscillator (HO) wave functions containing 15 major shells for all nuclei. For each nucleus, the value of the parameter $\hbar\omega$ of the HO basis is taken as the one minimizing the HF total nuclear energy.

The RPA equations are solved in matrix form in the p-h representation. RPA energies do not appear very sensitive to the value adopted for the HO parameter of the basis. For instance, by changing the optimal HF value $\hbar\omega = 8.7$ MeV in ^{208}Pb by 10%, the variation of the IS-
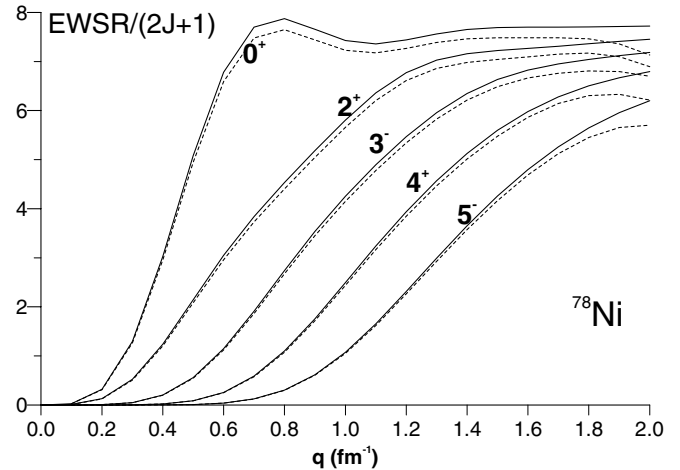
Fig. 1. Comparisons between the exact EWSR of eq. (3) (solid line) and those deduced from eq. (2) (dotted line) in ^{78}Ni for the RPA states with $J^\pi = 0^+$, 2^+, 3^-, 4^+ and 5^-. The unit of the EWSR scale is e^2 MeV. The abscissa q represents the transferred momentum.

GMR energy (13.46 MeV) is less than 0.5% and the energy of the first 2^+ at 4.609 MeV is changed by less than 5 keV.

Electric transition operators are defined according to

$$\widehat{Q}_{JM} = \frac{e}{2} \sum_i^A (1 - \tau_z(i)) \, j_J(qr_i) \, Y_{JM}(\theta_i, \phi_i), \quad (1)$$

where j_J is a spherical Bessel function of order J, q a transferred momentum, τ_z the third component of the nucleon isospin and Y_{JM} the usual spherical harmonics.

The degree of collectivity of the excited states is measured from their contribution to the Energy-Weighted Sum Rule (EWSR)

$$M_1(\widehat{Q}_{JM}) = \sum_N (E_N - E_0)|\langle N|\widehat{Q}_{JM}|0\rangle|^2, \quad (2)$$

where $|0\rangle$ and $|N\rangle$ are the RPA correlated ground state and excited states, respectively and $E_N - E_0$ their excitation energies. Equation (2) can also be expressed as the average in the HF ground state $|HF\rangle$ of a double commutator [15]:

$$M_1(\widehat{Q}_{JM}) = \frac{1}{2}\langle HF| \left[\widehat{Q}_{JM}, \left[\widehat{H}, \widehat{Q}_{JM}\right]\right] |HF\rangle. \quad (3)$$

Therefore, exact values of $M_1(\widehat{Q}_{JM})$ can be computed from expression (3), whereas smaller values will be obtained from (2), reflecting the finiteness of the particle-hole space used in the RPA calculations.

A comparison between the values calculated from (2) and (3) is shown in fig. 1 for ^{78}Ni as an example.

As can be seen, with the 15-major-shell basis employed, RPA calculations are able to describe with a reasonable accuracy the nuclear response for $J^\pi = 0^+$, 2^+, 3^-, 4^+ and 5^- up to transferred momenta $q = 1.5$ fm^{-1}.
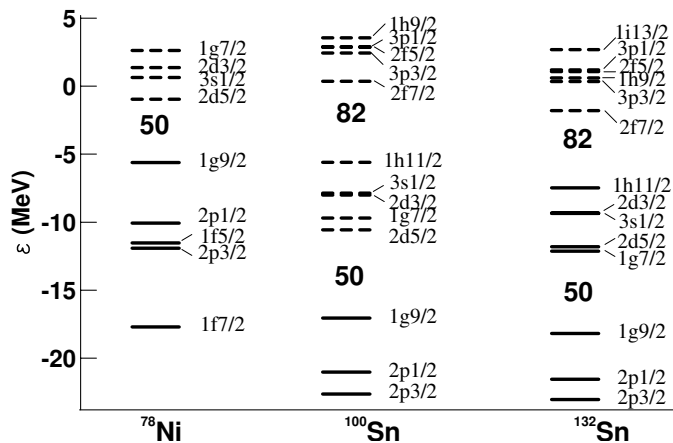
Fig. 2. Single-particle levels in the vicinity of the Fermi surface for neutrons in the three studied exotic nuclei. Filled and empty levels are represented by full and dashed lines, respectively. The labels indicate the quantum numbers (nlj) of the levels.

3 Results

First, we will discuss the validity of the doubly magic nature of these exotic nuclei. The single-particle neutron spectra obtained in ^{78}Ni, ^{100}Sn and ^{132}Sn are shown in fig. 2.

The $N = 50$ gap in ^{78}Ni and ^{100}Sn and the $N = 82$ one in ^{132}Sn are of the order of 5 MeV, which is less than 20% smaller than the gaps obtained for stable spherical nuclei with same neutron numbers. The same is true for the proton gaps at $Z = 28$ in ^{78}Ni and at $Z = 50$ in tin isotopes. That is, no significant reduction of the magic gaps are observed in these nuclei. Therefore, the three exotic nuclei are still doubly magic ones and the HF + RPA method is applicable to them.

In what follows, results for states with multipolarities 0^+, 2^+, 1^- and 3^- are presented for four nuclei, ^{78}Ni, ^{100}Sn ^{132}Sn and ^{208}Pb, the latter nucleus being included as a reference.

The strengths shown in the figures are given in percentage of the EWSR calculated in the long wavelength limit $q \to 0$. The relevant formulas to be used in this limit for the different values of J are given in the appendix of ref. [10].

In the present calculations the continuum spectrum of the HF Hamiltonian is approximated by a discrete one. As a consequence, the RPA strength functions appear in the form of discrete peaks. In order to make comparisons with experiments more meaningful, energy centroids will be defined in terms of the moments,

$$M_k \left(\widehat{Q}_{JM} \right) = \sum_N (E_N - E_0)^k |\langle N|\widehat{Q}_{JM}|0\rangle|^2 , \quad (4)$$

of the strength function. Two of these centroids will be used in the following: the mean value of the energy M_1/M_0, and the so-called "hydrodynamic" energy $\sqrt{M_1/M_{-1}}$ for isoscalar monopole resonances.

As experimental data on GR energies is scarce in exotic nuclei, comparisons will often be made with the system-
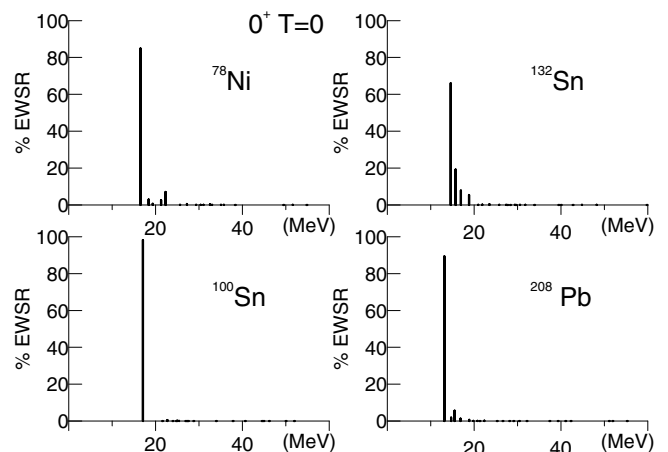
Fig. 3. Fraction of the EWSR carried by isoscalar $J^\pi = 0^+$ states in the four studied nuclei.

Table 1. Mean values and "hydrodynamic" centroids of IS-GMR energies in MeV obtained with the D1S$'$ force in the four studied nuclei compared with the empirical $80A^{-1/3}$ law and the ^{208}Pb experimental value from ref. [17].

0^+ $T = 0$	$\dfrac{M_1}{M_0}$	$\sqrt{\dfrac{M_1}{M_{-1}}}$	$80A^{-1/3}$	Exp.
^{78}Ni	17.17	17.07	18.72	
^{100}Sn	17.22	17.18	17.23	
^{132}Sn	15.29	15.22	15.72	
^{208}Pb	13.46	13.42	13.50	14.17 ± 0.28

atic $A^{-1/3}$ empirical laws approximately verified in stable nuclei [2]. Values from these systematics as well as available experimental data are given in the tables.

3.1 Monopole states

Figure 3 and table 1 display the results obtained for the Isoscalar Giant Monopole Resonance (ISGMR).

As is well known, the excitation energies of this resonance strongly depends on the compression modulus K_{nm} calculated in infinite nuclear matter [16]. One observes in table 1 that the theoretical energies in ^{208}Pb, although in good agreement with the empirical $80A^{-1/3}$ law, are 5% lower than the experimental value of ref. [17]. This difference is consistent with the compression modulus found in infinite nuclear matter with D1S$'$, $K_{nm} = 209$ MeV, which is slightly outside the interval 220–235 MeV that explains the bulk of experimental data within non-relativistic approaches [18].

Concerning the three exotic nuclei, we note that resonance energies significantly differ from the empirical law only in ^{78}Ni. It must be noted that, of all three nuclei, ^{78}Ni is the one where the squared neutron-proton asymetry $((N-Z)/A)^2$ most differs from the one of the stable isotope: $((N-Z)/A)^2 - ((N-Z)/A)^2_{stable} = 0.78$, 0.36 and -0.23 in ^{78}Ni, ^{132}Sn and ^{100}Sn, respectively. It is therefore

Table 2. Mean ISGMR energies in MeV obtained by leaving out from the D1S′ p-h interaction: (1) the spin-orbit and the Coulomb terms, (2) the Coulomb term, (3) the spin-orbit term, (tot) no term.

M_1/M_0	(1)	(2)	(3)	(tot)
^{78}Ni	18.55	17.10	18.59	17.17
^{100}Sn	18.19	16.81	18.54	17.22
^{132}Sn	16.07	15.06	16.26	15.29
^{208}Pb	13.73	13.05	14.10	13.46

tempting to correlate the $\simeq 1.5$ MeV lowering of the ISGMR found in ^{78}Ni with this large neutron excess, the contribution of the symmetry term K_{sym} to the finite nucleus incompressibility K_A being negative [19,20].

The strengths displayed in fig. 3 show that the major part of the EWSR is concentrated in a single peak in all four nuclei. This feature explains why the two sets of theoretical energies listed in table 1 are very close to each other. One notes that the fragmentation of the strength is almost zero in the $N = Z$ nucleus ^{100}Sn, whereas it is slightly bigger in the other three nuclei which have neutron-proton asymmetry $(N - Z)/A$ in the range 0.21–0.28.

In table 2, we show the values of the mean monopole energies M_1/M_0 obtained when different terms of the residual particle-hole (p-h) interaction are left out of the RPA calculation. Columns (1), (2) and (3) refer to the mean energies calculated by leaving out the spin-orbit and the Coulomb terms, the Coulomb term and the spin-orbit term, respectively.

One observes that the spin-orbit part of the residual interaction gives a contribution to ISGMR energies ranging from 8% in ^{78}Ni to 5% in ^{208}Pb. In contrast, the Coulomb contribution is larger in Pb (3%) and almost negligible in Ni. These results are consistent with those discussed in ref. [18] where ^{40}Ca, ^{90}Zr and ^{208}Pb were analyzed with the SLy4 interaction. In the latter work, the inclusion in the constrained HF (CHF) of the Coulomb force and of the spin-orbit component of the Skyrme interaction was proved to be essential in order to reconcile the value of K_{nm} obtained with the Skyrme and Gogny forces.

3.2 Quadrupole states

Figure 4 and tables 3, 4 and 5 display the results obtained for isoscalar quadrupole states. Figure 4 shows that in all four nuclei the quadrupole strength is divided essentially between two states: the isoscalar Giant Quadrupole Resonance (ISGQR) exhausting $\simeq 80\%$ of the EWSR with an energy in the range 12–16 MeV and a lower-lying state at $\simeq 3$–5 MeV carrying $\simeq 10\%$–15% of the quadrupole strength. We will label the latter 2_1^+.

The theoretical ISGQR energies are calculated using M_1/M_0 excluding the 2_1^+ state. The results shown in table 3 are seen to be higher than the $A^{-1/3}$ systematics by 1.0–1.5 MeV. As the latter agrees well with the
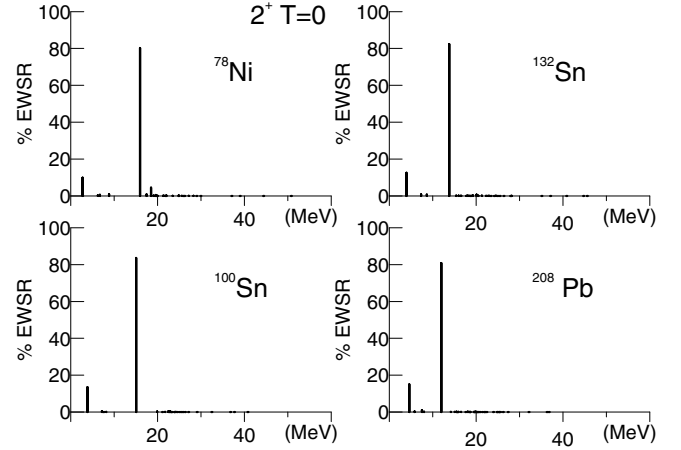
Fig. 4. Fraction of the EWSR carried by isoscalar $J^\pi = 2^+$ states in the four studied nuclei.

Table 3. Mean values of ISGQR energies in MeV obtained with D1S′ in the four studied nuclei compared with the empirical $64A^{-1/3}$ law and the ^{208}Pb experimental value from ref. [2].

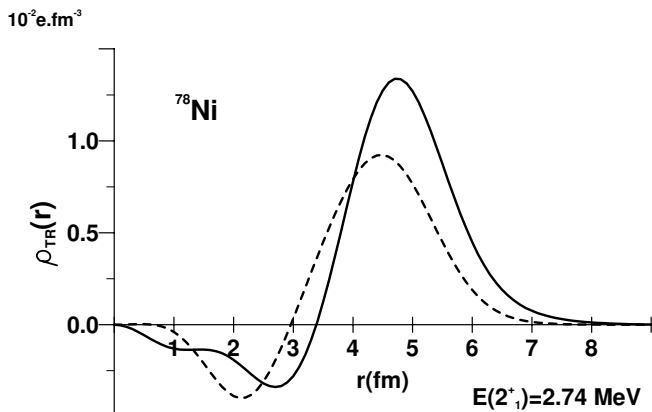| ISGQR	D1S′	$64A^{-1/3}$	Exp.
^{78}Ni	15.94	14.98	
^{100}Sn	15.13	13.79	
^{132}Sn	13.79	12.57	
^{208}Pb	11.98	10.80	10.60

Table 4. Energies in MeV and corresponding $B(E2)$ in e²fm⁴ of 2_1^+ states calculated with the D1S′ interaction. Existing experimental data from refs. [24] and [25] are also listed.

			Experiment	
2_1^+	E	$B(E2)$	E (MeV)	$B(E2)$
^{78}Ni	2.73	466		
^{100}Sn	3.84	1431		
^{132}Sn	3.97	1134	4.041	1400 (600)
^{208}Pb	4.609	2781	4.08	3180 (160)

experimental value in ^{208}Pb, it is difficult to draw definite conclusions concerning the behaviour of our results in the three exotic nuclei. Let us mention that such large ISGQR energies can be understood from a too large spreading of the particle-hole spectrum in the 2^+ channel at high energies. Such spreading is a consequence of the value of the effective mass of the D1S′ interaction ($m^*/m = 0.7$) which is the one giving correct single-particle properties in mean-field calculations. As is well known, taking into account the coupling of RPA configurations to 2-particle–2-hole (2p-2h) states would reduce this disagreement [21, 22]. Clearly, such a coupling should be introduced in the present calculations before reliable predictions for the ISGQR in exotic nuclei can be made [23]. Let us mention that the same is true for the other giant resonances, with some dependence on the mode quantum numbers [22].

Table 5. Energies in MeV and $B(E2)$ of 2_1^+ states obtained by leaving out from the D1S′ p-h interaction: (1) the spin-orbit and the Coulomb terms, (2) the Coulomb term, (3) the spin-orbit term, (tot) no term.
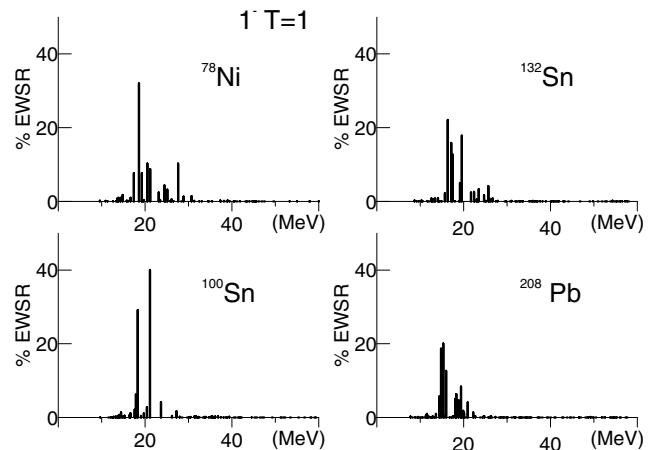
2_1^+	(1)		(2)		(3)		(tot)	
	E	$B(E2)$	E	$B(E2)$	E	$B(E2)$	E	$B(E2)$
^{78}Ni	3.53	257	2.84	456	3.43	271	2.73	466
^{100}Sn	4.64	1103	3.95	1552	4.48	1041	3.84	1431
^{132}Sn	4.61	775	4.04	1182	4.53	770	3.97	1134
^{208}Pb	5.15	2305	4.65	3145	5.09	2123	4.61	2781

Fig. 5. Neutron (full line) and proton (dashed line) transition densities for the first 2^+ state in ^{78}Ni.

Fig. 6. Fraction of the EWSR carried by isovector $J^\pi = 1^-$ states in the four studied nuclei.

Table 6. Mean values of IVGDR energies in MeV obtained with D1S′ in the four studied nuclei compared with the empirical $79A^{-1/3}$ law and the ^{208}Pb experimental value from ref. [28].

IVGDR	D1S′	$79A^{-1/3}$	Exp.
^{78}Ni	20.31	18.49	
^{100}Sn	19.98	17.02	
^{132}Sn	18.33	15.52	
^{208}Pb	16.50	13.33	13.43

Nevertheless, few results have been obtained up to now with such a coupling and it is difficult to foresee the magnitude of energy shifts, except for quadrupole and dipole states.

Our theoretical results for low-lying 2_1^+ states are presented in table 4. For these states, experimental data exist both for ^{208}Pb [24] and ^{132}Sn [25]. As can be seen, a fair agreement between experiment and theory is found in ^{208}Pb and an even better one in ^{132}Sn, with $B(E2)$ values being of the same order of magnitude as experimental ones. It is to be noted that we use the bare nucleon charges because no inert core is assumed. Let us point out that QRPA calculations applied to quadrupole states have been made recently with the D1S interaction for a series of tin isotopes including ^{132}Sn [13]. In these calculations, the spin-orbit part and the Coulomb part of the residual interaction were omitted for simplicity reasons. The 2^+ energies were found larger than the experimental ones by 400 keV in ^{102}Sn and 1 Mev in ^{132}Sn. The corresponding theoretical $B(E2)$ values were lower than experimental ones by at least a factor of two.

These results are consistent with those shown in table 5 where the same quantities as those of table 4 are displayed. They have been calculated by leaving out from the D1S′ p-h interaction the spin-orbit and the Coulomb terms, the Coulomb term, the spin-orbit term and no term, respectively. One observes that, as previously for monopole vibrations, taking into account the spin-orbit part of the residual interaction is essential to get results consistent with experimental data.

Going back to table 4, 2_1^+ energies are similar in ^{100}Sn and ^{132}Sn, whereas a comparatively low value is predicted in ^{78}Ni. Let us note that the 2_1^+ state in ^{78}Ni is still higher than the one in ^{56}Ni, the other doubly magic Ni isotope, where the experimental value of the 2_1^+ state is 2.7 MeV and the RPA calculated one is 2.42 MeV with D1S′.

The collectivity of this 2^+ state appears larger in ^{100}Sn than in ^{132}Sn and rather weak in ^{78}Ni. Figure 5 displays the transition density ρ_{TR} of this first 2_1^+ state in ^{78}Ni. The definition of the transition density is the same as the one given in the appendix of ref. [10].

One observes that the two transition densities are in phase and that the neutron transition density is higher than the proton one and displaced to a larger radius. This mode can therefore be interpreted as an isoscalar surface mode dominated by neutron excitation.

Table 7. Mean IVGDR energies in MeV and EWSR in TRK units for ^{208}Pb calculated by leaving out from the D1S′ p-h interaction: (1) the spin-orbit and the Coulomb terms, (2) the Coulomb term, (3) the spin-orbit term, (tot) no term. The three lines show the results obtained for the three energy intervals given in MeV in the leftmost columm. The rightmost column gives experimental EWSR in TRK units.

^{208}Pb	(1)		(2)		(3)		(tot)		Exp.
	$\langle E \rangle$	EWSR	$\langle E \rangle$	EWSR	$\langle E \rangle$	EWSR	$\langle E \rangle$	EWSR	EWSR
[0–140]	15.88	1.63	15.70	1.62	16.71	1.59	16.50	1.59	1.78
[0–20]	15.10	1.41	15.31	1.47	15.83	1.33	15.86	1.42	
[10–20]	15.20	1.39	15.17	1.49	15.90	1.32	15.95	1.41	1.37

3.3 Dipole states

Results for the isovector dipole resonance (IVGDR) are presented in fig. 6 and table 6.

^{100}Sn is the nucleus where the giant dipole mode is the least fragmented with 70% of the strength concentrated into two peaks. The dipole responses of ^{208}Pb and ^{132}Sn and, to a lesser extent, of ^{78}Ni also appear concentrated into two main energy regions. It is expected that the fragmentation is somewhat reduced by the coupling of the RPA modes to 2p-2h states, producing smoother strength functions, as in refs. [26,27] where Skyrme forces were used.

In ^{100}Sn the mean value $M_1/M_0 = 19.98$ MeV is 3 MeV larger than the systematic $79A^{-1/3}$ law (17.02 MeV). The EWSR value given in Thomas-Reiche-Kuhn (TRK) unit is 1.59, which is large compared to typical experimental values [28]. The IVGDR in ^{132}Sn is more fragmented than in ^{100}Sn. As in ^{100}Sn the mean energy value, 18.33 MeV, is much larger than systematics ($79A^{-1/3} = 15.52$ MeV) and the EWSR value is 1.58. In the case of ^{78}Ni, the IVGDR is quite fragmented with one major peak and smaller ones at higher energy. The mean energy value, 20.31 MeV, remains higher than systematics ($79A^{-1/3} = 18.49$ MeV) and the EWSR in TRK unit is 1.57.

It must be said that IVGDR excitation energies calculated with the Gogny force usually overestimate experimental data. In the case of ^{208}Pb, the calculated mean value is 16.50 MeV, which is quite large compared to experiment (13.43 MeV [28]), but smaller than the result of ref. [10]. Let us note that ignoring the higher part of the IVGDR response by keeping only the strength around the main lower energy peak, considerably improves the agreement with systematic estimations: mean energy values become 19.28 MeV, 18.16 MeV, 16.81 MeV and 14.99 MeV in ^{78}Ni, ^{100}Sn, ^{132}Sn and ^{208}Pb, respectively.

In fact, calculated IVGDR energies and EWSR appear quite sensitive to the energy interval considered and also to the components of the effective interaction included in the p-h residual interaction. This is shown in table 7 where mean IVGDR energies and EWSR in ^{208}Pb are listed for three energy integration intervals and for RPA calculations where Coulomb and/or spin-orbit terms are not included in the RPA matrix elements. One can see that the overestimation obtained with the Gogny force decreases by $\simeq$ 700 keV when the Coulomb and the spin-orbit forces are ignored, which is usually done in RPA calculations

Table 8. Energy in keV of the isoscalar 1^-_{sp} spurious state calculated by leaving out from the D1S′ p-h interaction: (1) the spin-orbit and the Coulomb terms, (2) the Coulomb term, (3) the spin-orbit term, (tot) no term. The symbol $\in \Im$ means that the RPA eigenvalue is imaginary.

| 1^-_{sp} $T = 0$	(1)	(2)	(3)	(tot)
^{132}Sn	$\in \Im$	$\in \Im$	2205.78	4.26
^{208}Pb	$\in \Im$	$\in \Im$	1605.19	2.29

employing Skyrme forces, see, however, ref. [29]. By taking all the terms of the Gogny force and considering the largest energy interval, the calculated EWSR given is 1.59 in TRK units. This value is higher than the experimental one obtained for a 10–20 MeV energy interval (1.37) [28] but lower than the one obtained for an energy interval going up to 140 MeV (1.78) [30]. In this case, however, another mechanism, the "quasi-deuteron effect", is expected to play a major role in the photon absorption [30].

It is of great interest, beyond nuclear physics itself, to study the amount of excited low-lying dipole strength, that is the often called "pygmy" resonances. In terms of EWSR, we obtain much less than 1% strength below 10 MeV in Ni and Sn nuclei, and about that amount in ^{208}Pb. The result for Pb is in agreement with the data of ref. [31]. The absence of collective states in the low-lying region is at variance with the results of relativistic RPA calculations [7], but agrees with the arguing in ref. [6]. There, it is pointed out that the soft dipole strength should decrease in nuclei displaying a neutron skin, compared to that in light halo nuclei because of a more efficient coupling to the IVGDR. On the other hand, the coupling to 2p-2h can significantly increase the amount of low-lying strength [26,27].

By introducing a very small renormalization factor (1.01–1.03) of the residual interaction, the isoscalar spurious mode can be made to appear at zero frequency. This factor is introduced only in the $J^\pi = 1^-$ subspace. In table 8, the values of the energy of this state are shown as calculated with or without different parts of the D1S′ p-h interaction. For each nucleus the same renormalisation factor is used in the four cases. The symbol $\in \Im$ means that the RPA eigenvalue is imaginary. These results show, as expected, that the consistency between the HF field and the residual interaction is important for the treatment of the spurious states.

Table 9. Energies in MeV of the first 3^- state and corresponding $B(E3)$ in 10^6 e^{2}fm^6 calculated by leaving out from the D1S$'$ p-h interaction: (1) the spin-orbit and the Coulomb terms, (2) the Coulomb term, (3) the spin-orbit term, (tot) no term. Experimental data from ref. [32] is also listed.

3_1^-	(1)		(2)		(3)		(tot)		Exp.	
	E	$B(E3)$	E	$B(E3)$	E	$B(E3)$	E	$B(E3)$	E	$B(E3)$
^{78}Ni	7.95	0.170	7.80	0.221	7.87	0.181	7.70	0.231		
^{100}Sn	7.26	0.130	6.95	0.149	7.13	0.128	6.82	0.147		
^{132}Sn	5.78	0.123	5.60	0.139	5.72	0.124	5.53	0.140		
^{208}Pb	3.55	0.725	3.38	0.782	3.57	0.677	3.39	0.727	2.6	0.611 (120)
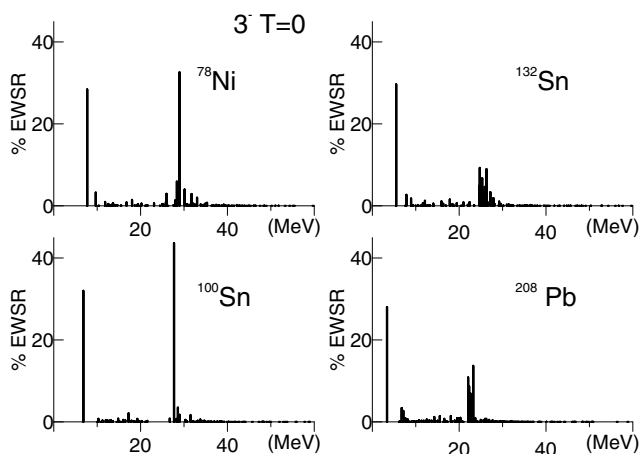
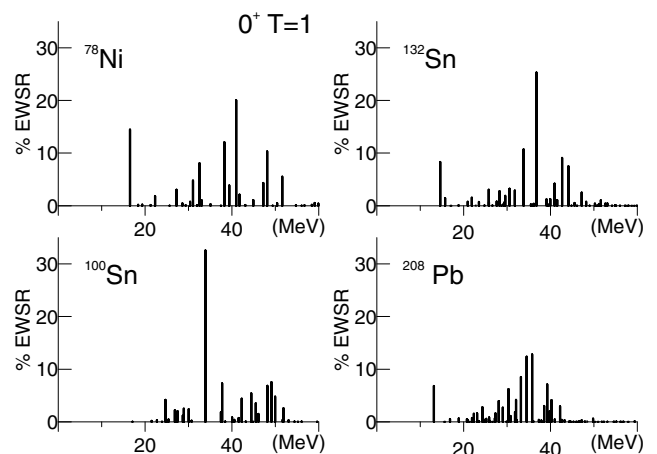**Fig. 7.** Fraction of the EWSR carried by isoscalar $J^\pi = 3^-$ states in the four studied nuclei.

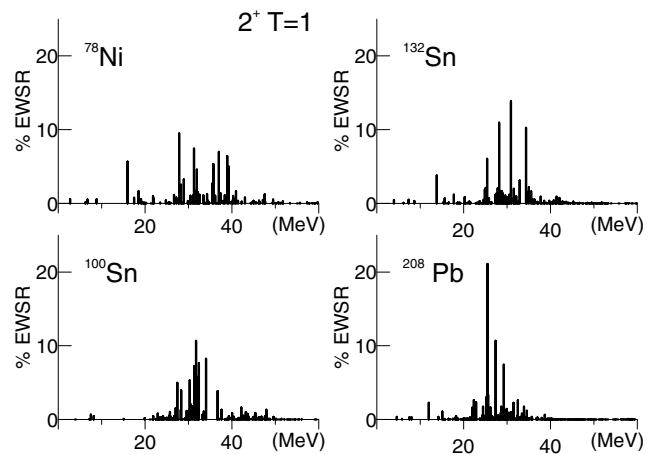**Fig. 8.** Fraction of the isovector EWSR carried by $J^\pi = 0^+$ states in the four nuclei.

3.4 Octupole states

As shown in fig. 7, the $J^\pi = 3^-$ states belong to two well-separated energy regions. Only the component at energies larger than $\simeq 15$ MeV can be considered as a genuine giant resonance, the High Energy Octupole Resonance (HEOR). Keeping only high-energy regions (19–35 MeV for ^{100}Sn, 22–31 MeV for ^{132}Sn, 22–44 MeV for ^{78}Ni and 13–28 MeV for ^{208}Pb), the mean calculated HEOR energies are 28.16 MeV, 26.06 MeV, 29.51 MeV and 23.20 MeV, respectively. These values give systematics $E_0 A^{-1/3}$, with E_0 = 130, 132, 126, and 137 in the four nuclei, to be compared with the usual estimate $110 A^{-1/3}$ [33]. Previous studies in stable nuclei [10] gave values between $130 A^{-1/3}$ and $140 A^{-1/3}$ for heavy nuclei and around $120 A^{-1/3}$ in lighter ones. We therefore do not observe a strongly different behaviour of HEOR energies in exotic nuclei compared to the one previously obtained along the valley of stability.

The characteristics of the low-energy 3^- states are reported in table 9. The influence of the different components of the D1S$'$ force included in the p-h interaction is also shown. The effect of the spin-orbit term appears to be smaller than for the quadrupole states in table 5, especially for ^{78}Ni.
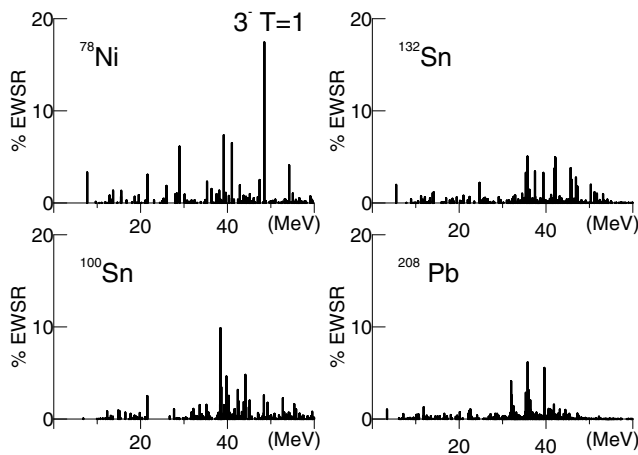

Fig. 9. Fraction of the isovector EWSR carried by $J^\pi = 2^+$ states in the four nuclei.

3.5 Isovector strength

In figs. 8–10, the fractions of the isovector EWSR carried by the $J^\pi = 0^+$, 2^+, 3^- states is drawn. In this case, systematics for stable nuclei are not yet well known [2] and is not reported.

Fig. 10. Fraction of the isovector EWSR carried by $J^\pi = 3^-$ states in the four nuclei.

Note that only the transition operator is changed compared to the isoscalar case in figs. 3, 4 and 7. From the comparison between the two sets of figures, a much larger fragmentation of the strength is found in the isovector case, and a mixed (isoscalar-isovector) character of several states appears, as expected, in particular in ^{78}Ni.

4 Conclusion

To summarize, we have presented the results obtained for different giant resonances in three doubly magic exotic nuclei, using the HF + RPA approach and the Gogny force. The largest difference with usual doubly magic nuclei inside the valley of stability occurs in ^{78}Ni where the ISGMR appears significantly lower than systematics. This seems to be due to the large proton-neutron asymmetry of this nucleus.

The fragmentation of the isovector dipole strength has to be explored further in order to see the correlation or the no-correlation with proton-neutron radius differences. In particular, the nature of the double peaks obtained in tin isotopes remains to be determined.

Results obtained in the three exotic nuclei for the IS-GQR and HEOR resonances are similar to those of ^{208}Pb, but more exotic systems have to be studied to confirm such a trend.

Low-energy states and $B(E2)$ values appear to be well reproduced within the present approach, in particular the first 2^+ one in ^{132}Sn.

From a more general point of view, we have found that the spin-orbit component of the p-h residual interaction plays a very important role in the structure of the low-lying quadrupole and octupole states, as it strongly influences both excitation energies and transition probabilities. Similarly, our results show that including the Coulomb force in the RPA p-h matrix elements significantly affects IVGDR energies and EWSR.

References

1. P.F. Bortignon, A. Bracco, R.A. Broglia, *Giant Resonances. Nuclear Structure at Finite Temperature* (Harwood Ac. Publ., New York, 1998).
2. M.N. Harakeh, A. van der Woude, *Giant Resonances: Fundamental High-energy Modes of Nuclear Excitation* (Oxford University Press, Oxford, 2001).
3. A. Leistenschneider *et al.*, Phys. Rev. Lett. **86**, 5442 (2001).
4. E. Tryggestad *et al.*, Phys. Rev. C **67**, 064309 (2003).
5. Cf., *e.g.*, O. Sorlin *et al.*, in *Proceedings of the International Conference on the Labirinth in Nuclear Structure*, AIP Conf. Proc. **701**, 31 (2004).
6. H. Sagawa, H. Esbensen, Nucl. Phys. A **693**, 448 (2001).
7. D. Vretenar, N. Paar, P. Ring, G.A. Lalazissis, Nucl. Phys. A **692**, 496 (2001).
8. J. Dechargé, D. Gogny, Phys. Rev. C **21**, 1568 (1980).
9. J.F. Berger, M. Girod, D. Gogny, Comput. Phys. Commun. **63**, 365 (1991).
10. J. Dechargé, L. Sips, Nucl. Phys. A **407**, 1 (1983).
11. J.P. Blaizot, D. Gogny, Nucl. Phys. A **284**, 429 (1977).
12. D. Gogny, J. Dechargé, J. Phys. (Paris), Colloq. **C4**, 221 (1984).
13. G. Giambrone *et al.*, Nucl. Phys. A **726**, 3 (2003).
14. S. Péru, J.F. Berger, Int. J. Mod. Phys. E **13**, 175 (2004).
15. E. Lipparini, S. Stringari, Phys. Rep. **175**, 103 (1989).
16. J.P. Blaizot, J.F. Berger, J. Dechargé, M. Girod, Nucl. Phys. A **591**, 435 (1995).
17. D.H. Youngblood, H.L. Clark, Y.-W. Lui, Phys. Rev. Lett. **82**, 691 (1999).
18. G. Colò, Nguyen Van Giai, Nucl. Phys. A **731**, 15 (2004).
19. G. Colò *et al.*, Phys. Rev. C **70**, 024307 (2004).
20. I. Hamamoto, H. Sagawa, X.Z. Zhang, Phys. Rev. C **56**, 3121 (1997); H. Sagawa, I. Hamamoto, X.Z. Zhang, J. Phys. G **24**, 1445 (1998).
21. P.F. Bortignon, R.A. Broglia, Nucl. Phys. A **371**, 405 (1981).
22. G.F. Bertsch, P.F. Bortignon, R.A. Broglia, Rev. Mod. Phys. **55**, 287 (1983).
23. F. Ghielmetti, G. Colò, P.F. Bortignon, R.A. Broglia, E. Vigezzi, Phys. Rev. C **54**, R2143 (1996).
24. J.F. Ziegler, G.A. Peterson, Phys. Rev. **165**, 1337 (1968); W.J. Vermeer *et al.*, Aust. J. Phys. **37**, 123 (1984).
25. J.R. Beene *et al.*, Nucl. Phys. A **746**, 471c (2004).
26. G. Colò, P.F. Bortignon, Nucl. Phys. A **696**, 427 (2001).
27. D. Sarchi, P.F. Bortignon, G. Colò, Phys. Lett. B **601**, 27 (2004).
28. B.L. Berman, S.C. Fultz, Rev. Mod. Phys. **47**, 713 (1975).
29. J. Terasaki *et al.*, Phys. Rev. C **71**, 034310 (2005)
30. A. Leprêtre *et al.*, Nucl. Phys. A **367**, 237 (1981).
31. N. Ryezayeva *et al.*, Phys. Rev. Lett. **89**, 272502 (2002).
32. R.H. Spear *et al.*, Phys. Lett. B **128**, 29 (1983).
33. F.E. Bertrand, Nucl. Phys. A **354**, 129c (1981).